

2.8 Parabolic Bottom

Up to this point we have dealt strictly with channels with rectangular cross-sections. The only allowable variation of bottom elevation has been in the longitudinal (y) direction. Although rectangular geometry lends mathematical convenience, it means that one must consider attached and detached flows separately. Were the two states dynamically similar, one might be content to put up with the implicit bookkeeping. The fact that there are significant differences raises some doubts concerning the artificial nature of rectangular geometry. For example, differences can be found in the dynamics of upstream disturbances; attached flow is controlled by Kelvin waves whereas detached flow is controlled by frontal waves. It has even been suggested that critical flow with respect to the latter can be difficult to achieve. A unifying theory taking into account the more realistic, rounded nature of natural straits would be quite advantageous. Such theory would allow a seamless merger between Kelvin and frontal wave dynamics. The simplest such model makes use of channel with a parabolic cross-section. Borenäs and Lundberg (1986, 1988) investigated this geometry for the case on finite, uniform potential vorticity and later zero potential vorticity. The following discussion is based largely on their work.

Consider a channel with bottom elevation:

$$h^*(x, y) = h^*(0, y) + \alpha(y)x^{*2},$$

nondimensionally

$$h(x, y) = h(0, y) + x^2 / r(y). \quad (2.8.1)$$

In the usual manner, D is used as a depth scale and $(gD)^{1/2}/f$ as a length scale. The parameter $r(y) = f^2 / g\alpha(y)$ can be interpreted as the ratio of the square of two length scales. The first is the half-width w_p of the level surface when the channel is filled evenly to a depth $d_p = \alpha w_p^2$ (Figure 2.8.1a). The second is a local Rossby radius of deformation $(gd_p)^{1/2} / f = (g\alpha)^{1/2} w_p / f$ based on this depth. Large values of r occur when the bottom curvature α is small compared to g/f^2 . As suggested in Figure 2.8.1a this is equivalent to a small local deformation radius $(gd_p)^{1/2} / f$ in comparison to the resting width $w_p = (d_p / \alpha)^{1/2}$. By the same measure, a dynamically narrow channel occurs when the curvature is large compared to g/f^2 (Figure 2.8.1b). That this measure of narrowness should depend only on the background parameters α , g , and f , and not fluid depth itself, is a special feature of the parabolic geometry and its uniform curvature.

The solution to (2.1.14) for the topographic profile (2.8.1) and for constant potential vorticity q can be written as

$$d(x, y) = \frac{1 + 2r^{-1}}{q \sinh q^{1/2}(a + b)} \left[\sinh q^{1/2}(x - b) - \sinh q^{1/2}(x + a) \right] + \frac{1 + 2r^{-1}}{q}. \quad (2.8.2a)$$

The corresponding geostrophic velocity is

$$v(x, y) = \frac{1 + 2r^{-1}}{q^{1/2} \sinh[q^{1/2}(a + b)]} \left\{ \cosh[q^{1/2}(x - b)] - \cosh[q^{1/2}(x + a)] \right\} + 2r^{-1}x. \quad (2.8.2b)$$

The surface or interface intersects the bottom at the two points $x=b$ and $x=-a$ (Figure 2.8.1c). The wetted width of the flow is therefore $a+b$.

In addition to the scales described above, the global deformation radius $(gD_{\infty})^{1/2} / f$ is present but hidden in arguments like $q^{1/2}(x + a) = (x^* + a^*)f / (gD_{\infty})^{1/2}$. As before, we might imagine that the potential depth D_{∞} is set in an upstream reservoir. If the range in x^* is large in comparison to $(gD_{\infty})^{1/2} / f$ at a particular section, the depth profile will have a boundary layer structure similar to that of the Gill (1977) model. If the range is small, arguments like $q^{1/2}(x - a)$ remain small, and the boundary layer structure is lost. The limiting case for the latter is the ‘zero potential vorticity’ limit, in which the fluid may be imagined to originate in a very deep, quiescent upstream basin.¹ It should be pointed out that the flow may still be ‘wide’ in the sense $\alpha \ll g/f^2$, as in Figure 2.8.1b, while remaining narrow in the sense $q^{1/2}(a + b) \ll 1$. The Denmark Strait sill has a value $r = g/f^2 \alpha$ of 10-20, based on the average value of α . The value of $q^{1/2}(a+b)$ based on observations cited in Nikolopoulos et al. (2003) ($D_{\infty}=600\text{m}$, $g=4.8 \times 10^{-3} \text{m/s}^2$, and $a^*+b^* \cong 50\text{km}$) is about 2.5.

The ‘zero potential vorticity’ case is the easiest to explore. The depth and velocity profiles may be obtained by taking the $q \rightarrow 0$ limit of (2.8.2), or simply by direct integration of (2.1.12) and (2.1.13) with $q=0$:

$$d = \frac{1}{2}(1 + 2r^{-1})(a + x)(b - x) \quad (2.8.3)$$

The accompanying velocity profile has constant shear

$$v(x) = -\left[x + \frac{1}{2}(1 + 2r^{-1})(a - b) \right] \quad (2.8.4)$$

The Bernoulli function

$$\frac{v^2}{2} + d + h(0, y) + \frac{x^2}{r} = \frac{D_{\infty}}{D}$$

¹ To be self consistent, the reservoir must have vertical side walls, else the depth would go to zero at the edges.

is uniform in the present limit. Substitution of (2.8.3) and (2.8.4) into this relation leads to

$$(1 + 2r^{-1}) \left[\frac{(a-b)^2}{r} + \frac{(a+b)^2}{2} \right] = 4\Delta z, \quad (2.8.5)$$

where $\Delta z = D_{\infty}/D - h(0, y)$ is the elevation of stagnant water in the upstream basin above the deepest point of the parabolic bottom.

The volume flux is found with the help of (2.8.5) to be

$$Q = \int_{-a}^b d(x)v(x)dx = \frac{(a+b)^3(2+r)}{6r^2} \left[\Delta z \frac{r^2}{2+r} - \frac{r(a+b)^2}{8} \right]^{1/2} \quad (2.8.6)$$

and the right-hand side has the required form for a hydraulic functional in the single variable $(a+b)$. Setting the derivative of this expression with respect to $(a+b)$ to zero leads to the critical condition. It can be verified in the usual manner that critical flow must occur at the sill and h must therefore be evaluated at the corresponding position $y=y_s$. The resulting critical condition is

$$(a+b) = \sqrt{\frac{6r\Delta z}{(2+r)}},$$

or, with the help of (2.8.5),

$$6(a-b)^2 = r(a+b)^2 \quad (2.8.7)$$

The corresponding controlled flux is given by

$$Q = \frac{\Delta z^2}{2+r} \sqrt{\frac{3r}{2}}, \quad (2.8.8)$$

or

$$Q^* = \frac{\Delta z^{*2}}{2+r} \sqrt{\frac{3g}{2\alpha}}. \quad (2.8.9)$$

This ‘weir’ formula can be compared with the case of a separated flow with rectangular cross-section (2.4.15) with the result

$$\frac{Q^*_{\text{parabolic}}}{Q^*_{\text{rectangular}}} = \frac{2}{(2+r)} \sqrt{\frac{3r}{2}}. \quad (2.8.10)$$

The comparison is meaningful for moderate or large values of r (wide channels) since the flow in the rectangular section is assumed to be separated. For large r it can be seen that the flux in the parabolic channel is less than the rectangular case by a factor proportional to $r^{-1/2}$. One of the reasons for this mismatch is that wide parabolic openings tend to favor reversals in velocity along the right edge, even when the flow is critical. In fact, it can be shown that flow reversals occur at the sill when $r > 2/3$.

The wide channel or weak curvature case ($r \gg 1$) can be developed a bit further by noting that (2.8.3) reduces to

$$d = \frac{1}{2}(a+x)(b-x).$$

The curvature of the interface is unity, dimensionally the Rossby radius based on the local depth. Such profiles tend to have flow and counterflow with positive velocity on the left and a return flow almost as great to the right (Figure 2.8.2). Since the velocity at the top of the profile is zero, the interface elevation must equal that in the quiescent upstream reservoir. All possible solutions for a given reservoir interface elevation are therefore found by simply sliding a parabola with fixed curvature and fixed maximum elevation back, as suggested in the figure. Upstream of the sill section, the profile must be centered slightly to the right of $x=0$ in order to achieve positive Q . At the shallower sill section, the interface profile is obtained by sliding the parabola to the right and this results in a weaker counterflow. Downstream of the sill, the parabola is slid further to the right and the resulting supercritical flow is unidirectional.

The existence of a counterflow at a critical (or supercritical) section would appear to confound the notion of upstream influence. Such flows seem to be sensitive downstream information despite the fact that no upstream wave propagation is possible. The situation may be made clearer by remembering that simple advection is quite different from propagation of mechanical information due to waves. One could place a drop of dye into a counterflow downstream of a controlling sill and follow its motion upstream and into the subcritical reaches of the current. However, the dye would not alter the transport or energy of the upstream flow, so there would be no real upstream influence. Rotating channel flows with counter currents are just one example of physically realizable, geophysically relevant flows that can have velocity reversals at the critical sections. Another example is the two-layer exchange flow (Chapter 5).

So far the discussion has revealed an important difference between the rectangular and rounded cases. Critical flow in a rectangular section must be unidirectional, provided the potential vorticity is uniform. At a parabolic section of sufficiently low curvature, critical flow will experience a velocity reversal and this leads to relatively small fluxes. Whether reversals actually occur at wide sills such as the Denmark Strait is not well

known; observations there suggest a stagnant region along the right edge (see Figure I8a).

We will discuss only a few aspects of the case of constant, non-zero potential vorticity. To begin with, the characteristic speeds are given by:

$$c_{\pm} = \hat{v} \pm \left\{ \alpha^2 T^{-2} (\hat{w} - 2Tq^{-1/2}) \left[\hat{w} - 2Tq^{-1/2} + (T^2 - 1) (\hat{w} - (1 + 2\alpha)T\alpha^{-1}q^{-1/2}) \right] \right\}^{1/2}. \quad (2.8.12)$$

(Pratt and Helfrich, 2005). Here $\hat{v} = \alpha(b - a)$, $T = \tanh(q^{1/2}\hat{w}/2)$ and $\hat{w} = a + b$. The corresponding Froude number

$$F_p^2 = \frac{T^2(b - a)^2}{(\hat{w} - 2Tq^{-1/2}) \left[\hat{w} - 2Tq^{-1/2} + (T^2 - 1) (\hat{w} - (1 + 2\alpha)T\alpha^{-1}q^{-1/2}) \right]} \quad (2.8.13)$$

can be useful in assessing the hydraulic criticality of an observed flow, provided that the potential vorticity q can be estimated and the bottom shape can be reasonably fit to a parabola. Girton et al. (*in press*) discuss an example of application to the Faroe Bank Channel. Equation (2.8.13) can also be guessed directly from the condition for steady, critical flow (Borenäs and Lundberg, 1986). Finally, we note that long wave speeds, Froude numbers and critical conditions for zero potential vorticity flow across a section of arbitrary topography can be written down. The derivation arises in the consideration of the stability of such flows and is presented in Section 3.9.

The differences between the zero- and finite-potential vorticity cases is particularly evident when the parabola is wide ($r \gg 1$). As shown by (2.8.3), the zero potential vorticity profile occupies a width $b+a$ that is comparable to the Rossby radius based on the maximum depth within the profile. On the other hand, a flow with finite potential vorticity (see 2.8.2a) may be spread over a much larger width. The interior of the depth profile consists of a wide region having constant depth q^{-1} , the nondimensional potential depth. The free surface or interface therefore parallels the bottom, implying a broad geostrophic flow with local velocity proportional to the cross-channel bottom slope. Where this slope is negative, the velocity is also so. The depth is brought to zero at the edges by boundary layers with width equal to the potential-depth based Rossby radius, nondimensionally $q^{-1/2}$. Negative flow occurs in the right-hand boundary layer.

Killworth (1992) has argued that the picture of a broad flow with a sluggish interior, high-velocity boundary layers, and flow reversals (Figure 2.8.3a) is characteristic of wide channels with more general shapes and potential vorticity distributions. Some of the elements of his elaborate argument are as follows. The channel is considered dynamically wide in the sense that changes in h with x occur over a scale much greater than boundary width scale $q^{-1/2}$. For this definition to have meaning, $q(\psi)$ must remain non-zero across the breadth of the flow. Now consider an upstream region in which the flow is sluggish ($v \ll 1$), so that $B(\psi) \cong d + h$ and $q(\psi) \cong 1/d$. It follows that, $d = d(\psi)$,

$h = h(\psi)$ and therefore $d=d(h)$, at least to a first approximation. The depth at any particular x in the interior region is therefore given by the potential depth $q^{-1}(\psi)$ for the value of ψ at that point. Since $d=d(h)$, the potential depth is determined by the local value of h . These features are characteristic of the *planetary geostrophic dynamics*, in which inertia is neglected but large variations in depth are allowed. In this limit, streamlines follow contours of constant h .

If streamlines originating in the sluggish region are followed downstream to the sill section, and if the topography remains gradually varying in x , then the streamlines will simply follow isobaths and the flow will remain sluggish. It is not possible, for example, for an isolated band of rapid geostrophic flow ($v=O(1)$, Figure 2.8.3b) to arise in the interior of the stream. There the geostrophic relation would require an $O(1)$ depth change, from d_1 to d_2 , over an distance $q^{-1/2}$, already assumed to be $O(1)$. However, the change in h across this distance is negligible for the assumed, gradually-varying topography, and thus the relation $d=d(h)$ is clearly violated. It therefore would seem that rapid bands of flow can only occur at the edges. The flow in the right-hand boundary layer will tend to be negative, since it must bring the depth to zero over a short distance.

It is not hard to construct examples of geostrophic flow across a broad sill that varies rapidly in the interior. The above arguments point out the difficulty in achieving such a state as the result of evolution from a slow, gradually varying upstream state.

Exercises

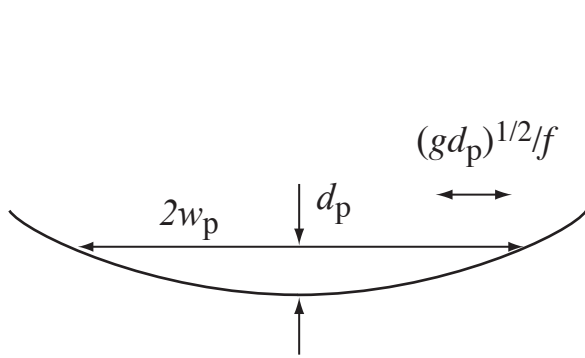
- 1) Compare the weir formula (2.8.9) to the case of attached, zero potential vorticity flow in a rectangular channel. Do the two formulas agree for $r \ll 1$? Should they?
- 2) Prove that a velocity reversal at a critical section with parabolic geometry and $q=0$ can only occur if $r > 2/3$.

Figure Captions

Figure 2.8.1 The narrow and wide limits of a parabolic channel.

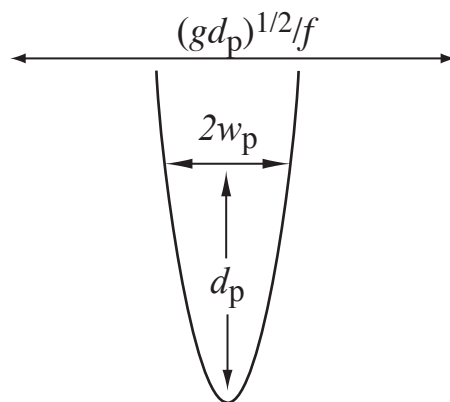
Figure 2.8.2 Example of zero potential vorticity flow in a wide parabolic channel at three sections. The upper thick curve represents the bottom at the sill section, whereas the lower thick curve represents the bottom at sections upstream and downstream of the sill. At the upstream section the subcritical solution (thinner curve) exists. Other solutions, including the critical solution at the sill and the supercritical solutions downstream, are obtained by sliding the parabola sideways. The apex of the parabola, where the velocity goes to zero, must remain at the same elevation.

Figure 2.8.3 (a) Slow across a section in which the topography varies gradually with x . The depth at each point is equal to the potential depth for that particular streamlines, and streamlines flow along contours of constant h . (b) A hypothetical band of flow with $v=O(1)$.



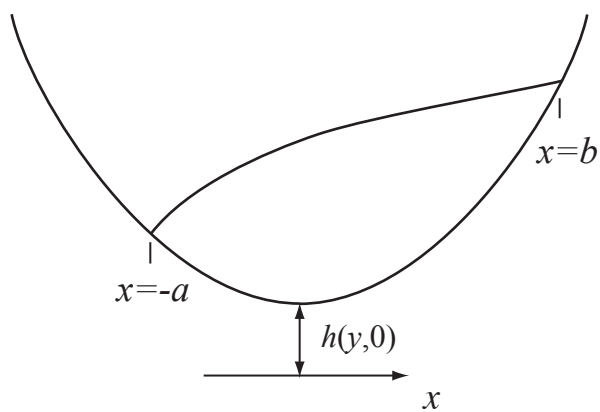
(b)

(wide channel)



(c)

(narrow channel)



(a)

Fig 2.8.1

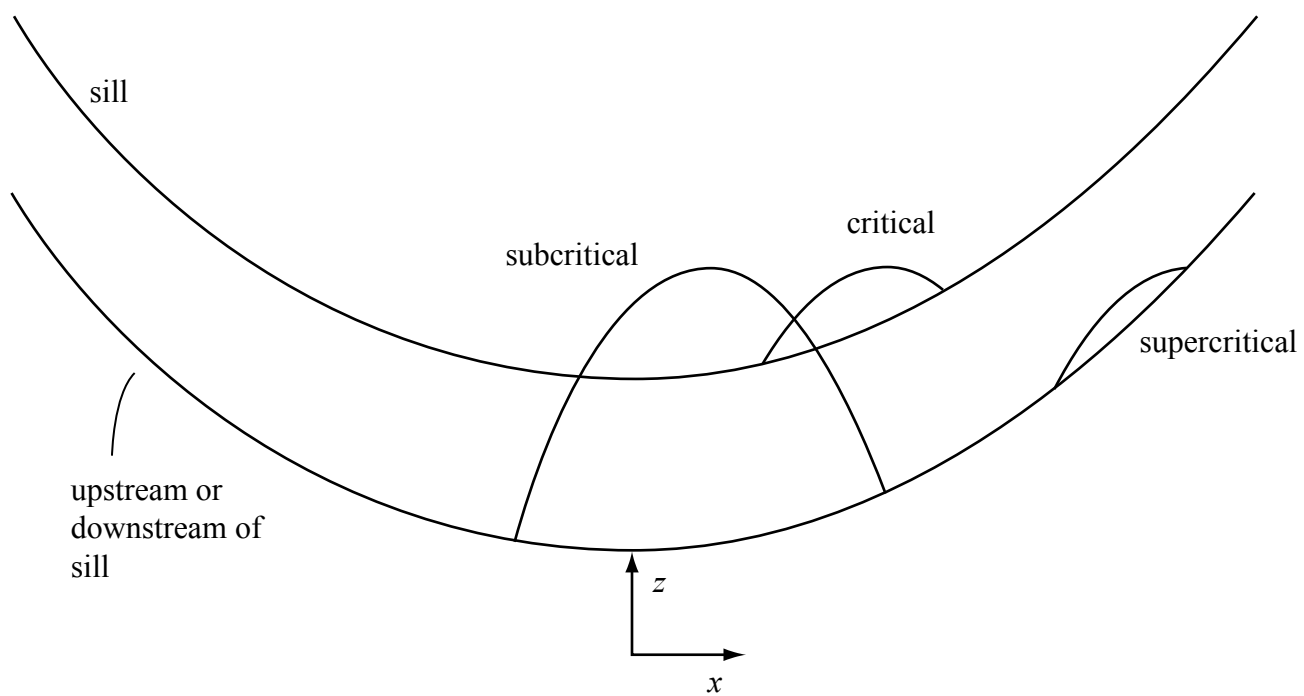


Figure 2.8.2

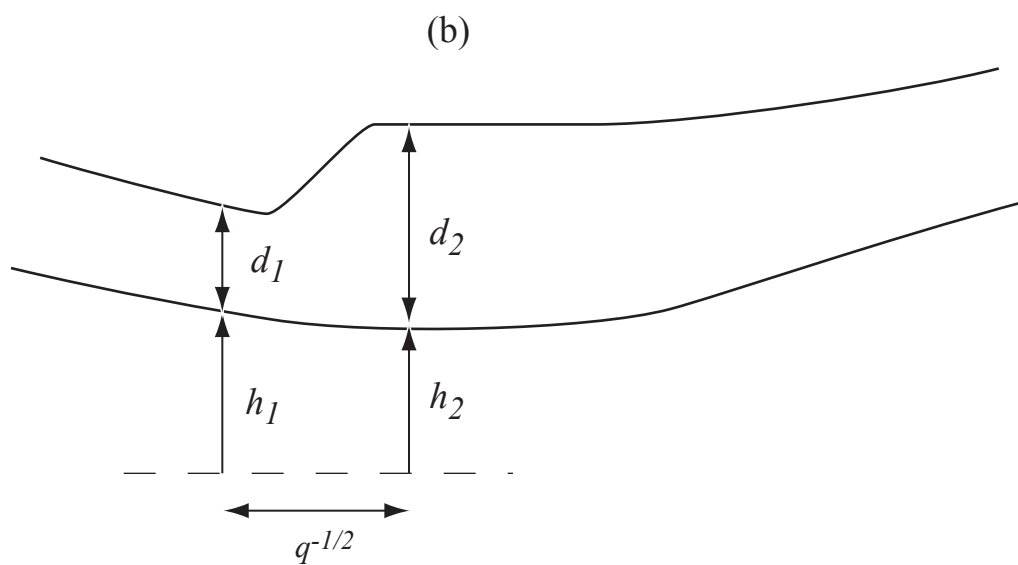
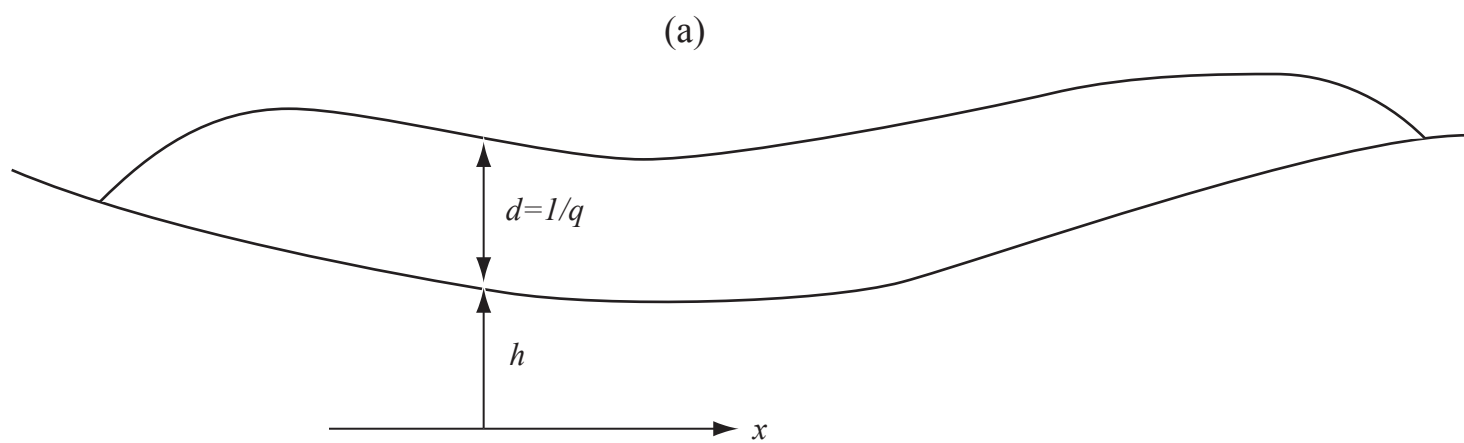


Figure 2.8.3